

# AC IMPEDANCE OF THE PERINEURIUM OF THE FROG SCIATIC NERVE

ANANDA WEERASURIYA

*Laboratory of Biophysics, National Institute of Neurological and Communicative Disorders and Stroke, National Institutes of Health, Bethesda, Maryland 20205*

ROBERT A. SPANGLER

*Department of Biophysical Sciences, State University of New York at Buffalo, Buffalo, New York 14214*

STANLEY I. RAPOPORT

*Laboratory of Neurosciences, National Institute on Aging, National Institutes of Health, Bethesda, Maryland 20205*

ROBERT E. TAYLOR

*Laboratory of Biophysics, National Institute of Neurological and Communicative Disorders and Stroke, National Institutes of Health, Bethesda, Maryland 20205*

**ABSTRACT** The AC impedance of the isolated perineurium of the frog sciatic nerve was examined at frequencies from 2 Hz to 100 kHz. A Nyquist plot of the imaginary and real components of the impedance demonstrated more than 1 capacitive element, and a DC resistance of  $478 \pm 34$  (SEM,  $n = 27$ )  $\Omega \text{ cm}^2$ . Transperineurial potential in the absence of externally applied current was  $0.0 \pm 0.5$  mV. The impedance data were fitted by nonlinear least squares to an equation representing the generalized impedance of four equivalent circuits each with two resistive and two capacitive elements. Only two of these circuits were consistent with perineurial morphology, however. In both, the perineurial cells were represented by a resistive and capacitive element in parallel, where capacitance was  $<0.1 \mu\text{F}/\text{cm}^2$ . The extracellular matrix and intercellular junctions of the perineurium were represented as single resistive and capacitive elements in parallel or in series, where capacitance exceeded  $2 \mu\text{F}/\text{cm}^2$ . Immersion of the perineurium in low conductance Ringer's solution increased DC resistive elements as compared with their values in isotonic Ringer's solution, whereas treatment for 10 min with a hypertonic Ringer's solution (containing an additional 1.0 or 2.0 mol NaCl/liter of solution) reduced DC resistive elements, consistent with changes in perineurial permeability. The results indicate that (a) perineurial impedance contains two time constants and can be analyzed in terms of contributions from cellular and extracellular elements, and (b) transperineurial DC resistance, which is intermediate between DC resistance for leaky and nonleaky epithelia, represents intercellular resistance and can be experimentally modified by hypertonicity.

## INTRODUCTION

Peripheral nerves of vertebrates are surrounded by a loose connective tissue sheath, the epineurium. Each nerve fascicle is bounded in turn by another more compact sheath, the perineurium, in which perineurial cells are arranged in one or more concentric layers, interspersed by collagen fibers (Thomas and Olsson, 1975; Low, 1976; Shinowara et al., 1982).

The vertebrate perineurium is a diffusion barrier which

restricts exchange of proteins, water-soluble nonelectrolytes and ions between the nerve environment (endoneurium) and epineurial extracellular space (Feng and Liu, 1949; Crescitelli, 1951; Krnjevic, 1954; Waggner et al., 1965; Olsson and Reese, 1971; Weerasuriya et al., 1979a, 1980). Together with endoneurial blood vessels, the system constitutes the blood-nerve barrier (Rapoport, 1976). Its barrier properties arise from tight junctions (*Zonulae occludentes*) that closely connect adjacent perineurial cells, and which in one or more of the inner perineurial layers, form networks of complete belts surrounding all of the cells so as to restrict intercellular diffusion (Burkel, 1967; Olsson and Reese, 1971; Reale et al., 1975; Akert et al., 1976; Shinowara et al., 1982).

---

Dr. Weerasuriya's present address is the Laboratory of Neurosciences, National Institute on Aging, National Institutes of Health, Bethesda, Maryland 20205.

Permeabilities of epithelial and other cell layers are considered to be related to cell overlap, to the number of tight junctions that connect the cells, and to the complexity and continuity of the tight junctional networks as seen with freeze fracturing (Frömter and Diamond, 1972; Claude and Goodenough, 1973; Lane, 1981; Crone and Olesen, 1982). On the basis of permeability to electron-dense tracers and to ions, and on the basis of the DC resistance, the leakiness of cell layers connected by tight junctions has been shown to vary by several orders of magnitude. For example, we recently found the permeability of the isolated perineurium of the frog sciatic nerve to  $\text{Na}^+$  to be  $1.7 \times 10^{-6} \text{ cm} \cdot \text{s}^{-1}$  (Weerasuriya et al., 1980), somewhat greater than the passive Na permeability of a nonleaky epithelium like the toad urinary bladder (Finn and Bright, 1978), but smaller than that of a leaky epithelium like the *Necturus* proximal tubule (Spring and Giebisch, 1977). On the other hand, the hydraulic conductivity ( $L_p$ ) of the perineurium is reported to equal  $0.75 \times 10^{-13} \text{ cm}^3 \cdot \text{s}^{-1} \cdot \text{dyn}^{-1}$  (Ask et al., 1983) as compared with values of  $0.35\text{--}0.88 \times 10^{-13} \text{ cm}^3 \cdot \text{s}^{-1} \cdot \text{dyn}^{-1}$  for nonleaky epithelia and  $1.8\text{--}4.4 \times 10^{-13} \text{ cm}^3 \cdot \text{s}^{-1} \cdot \text{dyn}^{-1}$  for leaky epithelia when measured at  $20^\circ\text{C}$  (Frömter and Diamond, 1972; Rapoport, 1976).

It is possible to further characterize cell layers by their electrical properties, which are related to ionic permeabilities. A low DC resistance, for example, characterizes a loose junctional intercellular network and a leaky epithelium (Frömter and Diamond, 1972; Claude and Goodenough, 1973). To further characterize the perineurium, we measured the AC impedance of the isolated perineurium by relating transverse current to transverse voltage at different frequencies, when the perineurial cylinder was immersed in isotonic Ringer's solution after exposure to hypertonic Ringer's solution, and in Ringer's solution of altered ionic strength. The data were analyzed in terms of a two-dispersion equivalent circuit that provided, among other things, estimates of the DC resistance of the intercellular matrix of the perineurium. A preliminary report of this work has been presented (Weerasuriya et al., 1979b).

## METHODS

Female *Rana pipiens* (Lake Champlain Frog Farm, Alburg, VT), ~9 cm long, were maintained in the laboratory at room temperature. An animal was double pithed and the sciatic nerve was removed from the spinal cord to the knee, with particular care to prevent stretching. As described previously (Weerasuriya et al., 1979a), under a dissecting microscope the perineurium was mobilized from underlying endoneurial tissue and rolled out over the cut end of the nerve. A cylindrical section, up to 18 mm long, was removed and mounted, as illustrated in Fig. 1, on two glass cannulae (0.65–0.70 mm, OD) that had fire-polished ends. The perineurium was mounted either in its normal orientation, or inverted, with the inside facing the bath. Perineurial diameter ranged from 0.65–0.80 mm and the exposed length was 8.0–11.0 mm.

The ends of the perineurium were sealed to the glass cannulae with a resinous cement (Grip cement, L. D. Caulk Co., Milford, DE). Each glass cannula was held in a Plexiglas block (shown in vertical cross section in Fig. 1) that contained a T-channel through which the perineurial cylinder

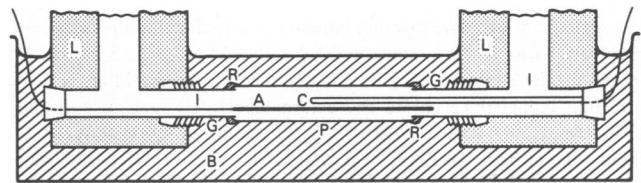


FIGURE 1 Experimental arrangement for measuring the AC impedance of the perineurium in vitro. A, current delivering Pt black axial wire; B, Ringer's solution bath; C, voltage measuring capillary electrode; G, glass cannulae; I, interior of the perineurial cylinder and Plexiglas blocks filled with Ringer's solution; L, Plexiglas blocks; P, Perineurium; R, resinous cement; S, Ag/AgCl wire.

could be perfused. With the electrode holders and glass cannulae in place, the electrical resistance of the leak at the horizontal ports exceeded 100 M $\Omega$ , thus ensuring effective electrical isolation of the solution within the perineurial cylinder from the outside bath. Each Plexiglas block was fixed rigidly to an aluminum rod, which, in turn, was attached to a micromanipulator.

The perineurium was perfused at a rate of ~0.13 ml/min. Solutions used were (a) isotonic Ringer's solution (115 mM NaCl, 2.5 mM KCl, 1.8 mM  $\text{CaCl}_2$ , 2.15 mM  $\text{Na}_2\text{HPO}_4$ , and 0.85 mM  $\text{NaH}_2\text{PO}_4$ ; osmolality = 220 mosmol/kg, pH = 7.2, and resistivity estimated at 90  $\Omega \text{ cm}$ ), (b) low-conductance Ringer's solution (Ringer's solution from which 90% of the NaCl was replaced by isosmotic amount of sucrose), pH = 7.2, osmolality = 220 mosmol/kg, and resistivity estimated at 660  $\Omega \text{ cm}$ , and (c) hypertonic Ringer's solution containing an additional 1.0 or 2.0 mol of NaCl/liter of solution, pH = 7.2. Solution temperature was maintained at  $21^\circ\text{--}22^\circ\text{C}$ .

## Impedance Measurements

The transperineurial potentials resulting from an imposed current of constant amplitude were measured at various frequencies by means of a phase-sensitive amplifier, yielding a direct indication of the real and imaginary components of the perineurial impedance. Fig. 1 illustrates the positions of the current and voltage electrodes relative to the perineurial cylinder, and Fig. 2 is the block diagram of electronic apparatus used for measuring impedance.

The electrical potential of the bathing solution immediately adjacent to the perineurium was clamped to virtual ground through the use of an operation amplifier. By this means, the magnitude of the AC signal seen by the relatively high impedance potential electrodes was reduced, correspondingly reducing the effect of stray capacitance in the potential

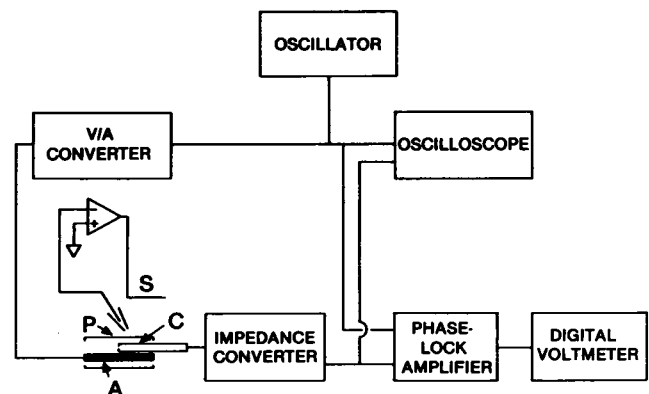


FIGURE 2 Circuit for measuring perineurial impedance. A, current delivering Pt black axial wire; C, voltage measuring capillary electrode; P, Perineurium; S, Ag/AgCl wire.

measuring circuits. The external potential electrode, comprising a chlorided silver wire in a micropipette filled with 3 M KCl, was located with its tip within 2 mm of the perineurium. The clamp amplifier, with its inverting input connected to the external potential sensing electrode, drove the external current electrode so as to maintain zero potential at its input. The current electrode, also Ag/AgCl, was located at least 4 cm from the perineurial preparation to provide as uniform a current distribution as possible along the length of the perineurium.

The internal current delivering electrode was an axial Pt/Pt black wire that extended the length of the perineurial cylinder, and delivered a sinusoidal current of constant amplitude supplied by a voltage-to-current converter driven by an oscillator (model 5200A, Krohn-Hite Corp., Avon, MA). The electrical potential within the perineurial cylinder was measured by means of a 3 M KCl-filled axial pipette with its tip drawn out to a diameter of  $\sim 30 \mu\text{m}$  and placed at about the midpoint of the preparation. The high frequency impedance of this pipette was reduced by an internal thin shiny Pt wire. This electrode, with a DC resistance varying from 0.2 to 1.5 M $\Omega$ , was connected to an impedance converter with a gain of 2. Its output in turn was led into the phase-lock amplifier (Ortholoc, model 9502, Brookdeal Electronics Ltd., Brookshire, England), with the oscillator output signal serving as the reference. The amplifier output was connected to a digital voltmeter that indicated the real and imaginary components of the impedance. Signals from the oscillator and the impedance converter were monitored continuously on an oscilloscope screen.

After perfusion of the perineurium was interrupted, the perineurial impedance was measured by varying the current frequency in 3 steps per decade between 2 Hz and 100 kHz. A complete set of measurements took  $\sim 6$  min. Current amplitude was kept below  $70 \mu\text{A}/\text{cm}^2$ , and was varied occasionally to ascertain that impedance was independent of amplitude and this criterion was used to assure that measurements were within the amplitude range of a linear response. The data were corrected for phase shifts and decrements of magnitude introduced by the electronic equipment and the electrodes, by repeating the experiments when the perineurium was removed. Largest phase shifts and decrements of magnitude occurred at high frequencies, with a maximum of  $5.3^\circ$  and 7%, respectively, at 100 kHz.

Current density along the perineurium was investigated by placing the tips of two KCl-filled micropipettes 0.7 mm apart, along a line normal to the cylindrical axis. These pipettes were connected to a high-impedance differential amplifier (Preamp Model 113, Princeton Applied Research, Princeton, NJ), from which the output, directly proportional to current density at the pipette tips, was fed into the phase-lock amplifier. As illustrated in Fig. 3, variation in current density at 2 Hz was negligible along the length of the perineurial cylinder, and phase variation also was insignificant. A nonuniform amplitude indicates some leakage at the ends, and this effect at 2 Hz might cause resistance to be underestimated by at most 15%. At higher frequencies, current density became more uniform and consequently errors arising from leakage were less significant. The DC resistance of the perineurium changed (usually a gradual decrease) by 10% or less in 40 min. In each experiment requiring changes in bathing solutions, the time required for the complete procedure did not exceed 30 min.

After the impedance of the perineurial cylinder was measured in Ringer's solution, the bathing solution was changed to examine the effects of solution conductivity or osmolarity upon the measured impedance. In any one experiment, bathing solutions were changed in one of two ways: (a) The bath and the solution inside the perineurial cylinder were replaced by a low-conductance Ringer's solution, in which 90% of the NaCl had been replaced by an isosmotic amount of sucrose. After a 10 min exposure to this low-conductance medium, the impedance of the perineurium was measured again. By monitoring the impedance at a few selected frequencies (5, 100, and 2,000 Hz) immediately after changing solutions, it was found that the impedance stabilized at a new, higher value within 8 min. (b) The bath but not the internal solution was replaced with a Ringer's solution, made hypertonic with NaCl, for a period of 10 min (in the absence of perfusion) after which the perineurium

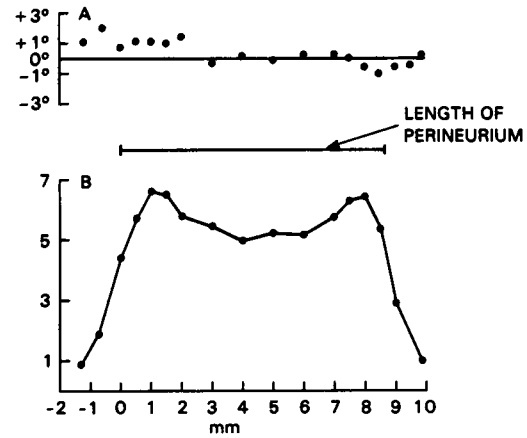


FIGURE 3 Variation in current density along the length of the perineurium. The current across the perineurium at a particular point is compared in phase (A) and magnitude (B) with the total current. The current was delivered as a 2 Hz sine wave.

was returned to the isotonic Ringer's solution, and the perineurial cylinder was perfused (at a rate of  $\sim 0.13 \text{ ml}/\text{min}$ ) with isotonic Ringer's solution for 5 min to replace the slightly hypertonic solution inside it. The impedance of the perineurium then was remeasured. Both the normal and inverted preparations were subjected to each of the two hypertonic soaks.

The impedance was measured as its imaginary and real component over the frequency range 2 Hz to 100 KHz. After the data had been corrected for the residual phase shift of the instruments (see above) they were analyzed by a nonlinear least-square curve-fitting technique (Knott, 1979). For an equivalent circuit with four elements (two resistors and two capacitors), there are four canonical combinations of such elements, excluding those forms with an infinite impedance at zero frequency (Fig. 4). In each of the canonical forms, the impedance can be represented by a ratio of complex numbers having the explicit frequency dependence shown in Eq. 1:

$$Z(\omega) = \frac{N_R + i\omega N_I}{1 - \omega^2 D_R + i\omega D_I} \quad (1)$$

In which  $i = \sqrt{-1}$  and  $\omega$  is the frequency in radians per second ( $\omega = 2\pi f$ ). The form-independent parameters,  $N_I$ ,  $N_R$ ,  $D_I$ , and  $D_R$  after

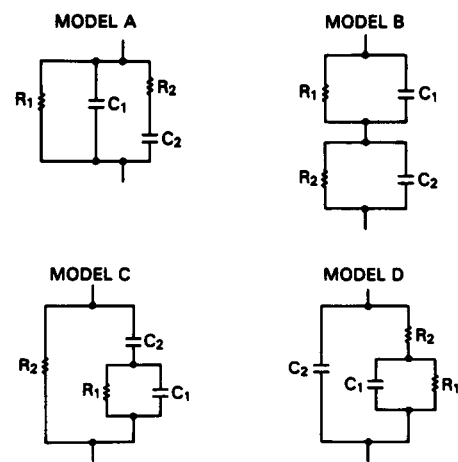


FIGURE 4 The four possible equivalent circuits for two resistors and two capacitors.

being fitted to the data, are used to compute the specific element values in each of the four canonical circuit forms. The relations between the circuit element values, and the form-independent parameters are given in Table I. The statistical computations were done using the method of paired comparison of the students *t* test.

## RESULTS

The Nyquist plot of the impedance of the frog perineurium has two distinct dispersions (Fig. 5), which indicate that there are at least two different time constants. Further, the voltage produced across the perineurium by the imposed current always had a phase lag (i.e., the imaginary component of the AC impedance was always negative). These two features suggest that the equivalent circuit for the perineurium has at least two capacitors and more than one resistor. Four possible canonical forms of an equivalent circuit with two capacitors and two resistors are shown in Fig. 4. The four parameters of each model were obtained from the impedance data according to the procedure described in the Methods section. Increasing the degrees of freedom of the models by the addition of a third resistor did not significantly enhance the fit but decreased its uniqueness (i.e., an equally close fit could be achieved by changing the values of two or more parameters in a dependent manner). Hence we limited our equivalent circuit analysis to the four element models illustrated in Fig. 4.

In models A and C, the DC resistance is  $R_1$  and  $R_2$ , respectively, whereas in models B and D the DC resistance is the sum of  $R_1$  and  $R_2$ . This similarity between A and C on the one hand and between B and D on the other is further exemplified by the values assigned to the components in each of the models.

The calculated mean DC resistance of the normal perineurium was  $478 \pm 34$  (SEM,  $n = 27$ )  $\Omega \text{ cm}^2$ . In this in vitro arrangement the transperineurial potential was  $0.0 \pm 0.5$  mV.

Replacing the Ringer's solution bath by a low-conduc-

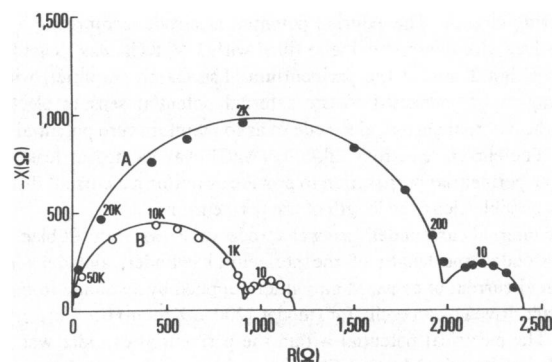


FIGURE 5 Impedance loci of perineurium of frog sciatic nerve under normal conditions (A) and after exposure to hypertonic (Ringer's solution + 1.0 M NaCl) solution (B). The abscissa is the real and the ordinate the imaginary component of the impedance in ohms. The imaginary part is plotted with the negative sign upwards. The numbers on the curves indicate the frequency in Hz.

tance medium (90% of NaCl substituted by an equiosmolal amount of sucrose) changed the calculated values of the resistors, whereas the values of the capacitors were not altered ( $P > 0.05$ ) (Table II). The calculated DC resistance ( $R_1$  in A,  $R_2$  in C, and  $R_1 + R_2$  in B and D) increased fivefold. The value of the smaller capacitance in all four models decreased in the low conductance medium although this decrease was not statistically significant.

Immersion of the perineurium in hypertonic Ringer's solution for 10 min decreased the DC resistance which was measured when the perineurium was returned to isotonic Ringer's solution (Tables III and IV). This decrease was related to the degree of hypertonicity. Exposure to 1.0 M NaCl hypertonicity decreased the estimated DC resistance by  $\sim 33\%$  and exposure to 2.0 M NaCl hypertonicity produced a decrease of  $\sim 70\%$ . The exposure time in both cases was 10 min. The lesser hypertonic medium did not significantly alter the capacitances in any of the models

TABLE I  
THE RELATIONS BETWEEN THE CIRCUIT ELEMENT VALUES OF THE  
FOUR CANONICAL FORMS AND THE FORM-INDEPENDENT PARAMETERS

	A	B	C	D
$R_1$	$N_R$	$\frac{N_R}{2} - \frac{2N_1 - N_R \cdot D_1}{2\sqrt{D_1^2 - 4D_R}}$	$\frac{N_1 \cdot N_R(D_1 \cdot N_R - N_1) - D_R \cdot N_R^2}{(D_1 \cdot N_R - N_1)^2}$	$\frac{N_R(D_1 \cdot N_1 - D_R \cdot N_R) - N_1^2}{D_1 \cdot N_1 - D_R \cdot N_R}$
$R_2$	$\frac{N_R \cdot N_1^2}{N_1(D_1 \cdot N_R - N_1) - D_R \cdot N_R^2}$	$\frac{N_R}{2} + \frac{2N_1 - N_R \cdot D_1}{2\sqrt{D_1^2 - 4D_R}}$	$N_R$	$\frac{N_1^2}{D_1 \cdot N_1 - D_R \cdot N_R}$
$C_1$	$\frac{D_R}{N_1}$	$\frac{2D_R \cdot \sqrt{D_1^2 - 4D_R}}{2N_R \cdot D_R - N_1(D_1 - \sqrt{D_1^2 - 4D_R})}$	$\frac{D_R(D_1 \cdot N_R - N_1)}{N_1(D_1 \cdot N_R - N_1) - D_R \cdot N_R^2}$	$\frac{(D_1 \cdot N_1 - D_R \cdot N_R)^2}{N_1 \cdot N_R(D_1 \cdot N_1 - N_R \cdot D_R) - N_1^2}$
$C_2$	$\frac{N_1(N_R \cdot D_1 - N_1) - D_R \cdot N_R^2}{N_R^2 \cdot N_1}$	$\frac{2D_R \cdot \sqrt{D_1^2 - 4D_R}}{N_1(D_1 + \sqrt{D_1^2 - 4D_R}) - 2N_R \cdot D_R}$	$\frac{D_1 \cdot N_R - N_1}{N_R^2}$	$\frac{D_R}{N_1}$

TABLE II  
EFFECT OF LOW-CONDUCTANCE MEDIUM  
(90% OF NaCl IN RINGER'S SOLUTION REPLACED WITH SUCROSE)

	A	B	C	D
$R_1$ ( $\Omega\text{cm}^2$ )	385 $\pm$ 84 1,948 $\pm$ 440*	108 $\pm$ 29 652 $\pm$ 130*	1,053 $\pm$ 290 4,513 $\pm$ 1,600	87 $\pm$ 23 538 $\pm$ 113*
$R_2$ ( $\Omega\text{cm}^2$ )	1,271 $\pm$ 256 5,558 $\pm$ 1534‡	277 $\pm$ 63 1,296 $\pm$ 368	385 $\pm$ 84 1,948 $\pm$ 440*	298 $\pm$ 62 1,410 $\pm$ 345
$C_1$ ( $\mu\text{F}/\text{cm}^2$ )	0.081 $\pm$ 0.007 0.069 $\pm$ 0.004	43.7 $\pm$ 17.6 32.6 $\pm$ 14.0	0.106 $\pm$ 0.022 0.091 $\pm$ 0.014	45.2 $\pm$ 17.5 33.4 $\pm$ 14.0
$C_2$ ( $\mu\text{F}/\text{cm}^2$ )	2.71 $\pm$ 1.45 2.35 $\pm$ 1.25	0.088 $\pm$ 0.010 0.078 $\pm$ 0.007	2.79 $\pm$ 1.45 2.42 $\pm$ 1.25	0.081 $\pm$ 0.007 0.069 $\pm$ 0.006

All values are expressed as mean  $\pm$  SEM,  $n = 6$ . In this and the following tables, the upper and lower figures in each set are the values before and after experimental manipulations, respectively.

\* $P < 0.01$ , ‡ $P < 0.05$ . All other values show no significant differences ( $P > 0.05$ ).

( $P > 0.1$ ). The 2.0 M NaCl hypertonic medium caused a significant increase in the value of the smaller capacitor ( $P < 0.01$ ). Fig. 5 graphically demonstrates the change in impedance produced by hypertonic treatment.

#### DISCUSSION

An AC impedance analysis of the electrical properties of the perineurium provides information with regard to the capacitative properties of the tissue and the number of time constants characteristic of the system as well as its resistive properties. The equivalent circuits used in the analysis were limited to four-element models containing two capacitors and two resistors. The inclusion of a third resistor in the circuits did not significantly improve the fits, but would only decrease the uniqueness of the values assigned to the form-independent parameters by the curve-fitting routine. The AC impedance analysis technique has been successfully used to measure the membrane properties of gastric mucosa (Clausen et al., 1983), electrical properties of the

rabbit urinary bladder (Clausen et al., 1979), capacitance of *Necturus* gall bladder (Schifferdecker and Frömter, 1978), capacitance and active transport in frog skin (Smith, 1975; Brown and Kastella, 1965), electrical properties of cardiac Purkinje strands (Freygang and Trautwein, 1970), longitudinal impedance of smooth muscle (Tomita, 1969), and electrical impedance of striated muscle (Fatt, 1964; Falk and Fatt, 1964; Adrian and Almers, 1974; Valdiosera et al., 1974).

Nyquist plots of experimental data clearly demonstrate the presence of more than one capacitative element in the perineurium (Fig. 5). Although each of the equivalent circuits in Fig. 4 provides an impedance given by Eq. 1, the appropriateness of each circuit can be evaluated in the light of perineurial ultrastructure. Analysis of the data in terms of each of four canonical equivalent circuits (Fig. 4) assigns a relatively invariant value of  $\sim 0.08 \mu\text{F}/\text{cm}^2$  to the smaller capacitor while the larger capacitance is more variable. Electron microscopic studies demonstrate the presence of six or more layers of cells in the perineurium of

TABLE III  
EFFECT OF EXPOSURE TO HYPERTONIC SOLUTION ( $R + 1.0 \text{ M NaCl}$ )

	A	B	C	D
$R_1$ ( $\Omega\text{cm}^2$ )	493 $\pm$ 70 330 $\pm$ 62*	155 $\pm$ 50 91 $\pm$ 39‡	1,587 $\pm$ 359 1,261 $\pm$ 261	102 $\pm$ 22 65 $\pm$ 15*
$R_2$ ( $\Omega\text{cm}^2$ )	2,168 $\pm$ 299 1,552 $\pm$ 289	338 $\pm$ 37 328 $\pm$ 29‡	493 $\pm$ 70 330 $\pm$ 62*	390 $\pm$ 54 265 $\pm$ 49*
$C_1$ ( $\mu\text{F}/\text{cm}^2$ )	0.075 $\pm$ 0.006 0.077 $\pm$ 0.007	202 $\pm$ 69.4 340 $\pm$ 80.3	0.104 $\pm$ 0.017 0.089 $\pm$ 0.012	201 $\pm$ 70.5 343 $\pm$ 81.0
$C_2$ ( $\mu\text{F}/\text{cm}^2$ )	5.12 $\pm$ 1.79 10.9 $\pm$ 2.92	0.083 $\pm$ 0.006 0.080 $\pm$ 0.007	5.19 $\pm$ 1.79 11.0 $\pm$ 2.93	0.075 $\pm$ 0.006 0.077 $\pm$ 0.007

All values are expressed as Mean  $\pm$  SEM,  $n = 9$ .

\* $P < 0.01$ , ‡ $P < 0.025$ . All other values show no significant differences ( $P > 0.05$ ).

TABLE IV  
EFFECT OF EXPOSURE TO HYPERTONIC SOLUTION ( $R + 2.0$  M NaCl)

	A	B	C	D
$R_1$ ( $\Omega\text{cm}^2$ )	515 $\pm$ 39 152 $\pm$ 20*	89 $\pm$ 13 39 $\pm$ 11*	2726 $\pm$ 330 616 $\pm$ 109*	89 $\pm$ 13 25 $\pm$ 5*
$R_2$ ( $\Omega\text{cm}^2$ )	2,814 $\pm$ 372 886 $\pm$ 121*	425 $\pm$ 32 113 $\pm$ 14*	515 $\pm$ 39 152 $\pm$ 20*	426 $\pm$ 32 127 $\pm$ 17*
$C_1$ ( $\mu\text{F}/\text{cm}^2$ )	0.088 $\pm$ 0.007 0.104 $\pm$ 0.007	787 $\pm$ 111 856 $\pm$ 252	0.089 $\pm$ 0.008 0.143 $\pm$ 0.015*	791 $\pm$ 111 860 $\pm$ 252
$C_2$ ( $\mu\text{F}/\text{cm}^2$ )	29.5 $\pm$ 8.56 16.4 $\pm$ 5.21	0.088 $\pm$ 0.007 0.115 $\pm$ 0.008*	29.6 $\pm$ 8.56 16.5 $\pm$ 5.22	0.088 $\pm$ 0.007 0.104 $\pm$ 0.007*

All values are expressed as Mean  $\pm$  SEM,  $n = 12$ .

\* $P < 0.01$ . All other values are not significantly different ( $P > 0.05$ ).

the frog sciatic nerve, and that the cell membranes of the perineurial cells frequently are folded and invaginated into calveoli (Shinowara et al., 1982). It is suggested therefore that the smaller capacitor represents the net capacitance of the six or more cell layers of the perineurium. Six layers of cells arranged in series with a capacitance of  $\sim 1.0 \mu\text{F}/\text{cm}^2$  at each cell membrane would have a total capacitance of  $\sim 0.08 \mu\text{F}/\text{cm}^2$ . On the other hand, more than six layers, with each cell membrane exhibiting some degree of folding and invagination, and thus having a larger capacitance per square centimeter, could account for a similar total capacitance.

With the transperineurial impedance measurement and equivalent circuit analysis, it is not possible to separate the resistance of the cell membranes from the parallel resistance of the junctions between adjacent cells of a given layer. Thus, the resistor in parallel with the smaller capacitor in each of the models represents the combined resistance of the cell membranes and the intercellular junctions.

In model A, if  $C_1$  represents the cell membrane capacitance, then  $R_1$  would include the cell membrane resistance. Intercellular junctions within a layer would be in parallel with the cell membranes of that layer. If  $C_1$  and part of  $R_1$  represent the cell membranes, the remainder of  $R_1$  as well as  $R_2$  and  $C_2$  may represent intercellular matrix and junctions. This interpretation is consistent with four- to fivefold elevations in both  $R_1$  and  $R_2$  in low conductance Ringer's solution (Table II), and with the decline in  $R_1$  and  $R_2$  when the perineurium was returned to isotonic Ringer's solution after exposure to hypertonic Ringer's solution (Tables III and IV). Such hypertonic treatment is known to increase perineurial permeability to the extracellular tracer,  $^{14}\text{C}$ -sucrose, which is consistent with these observations (Weerasuriya et al., 1979a). Because the smaller capacitances in the models, which probably represent the cell membrane capacitance (see above), were not eliminated by hypertonic exposure, the DC resistance probably fell because of increased paracellular shunting rather than

by cell disruption. In other epithelia, hypertonic exposure can decrease tissue DC resistance by altering junctional morphology (Rawlins et al., 1975; Eriij and Martinez-Palomo, 1972; Ussing, 1966). Calculated  $C_2$  for model A (2.7–29.5  $\mu\text{F}/\text{cm}^2$ ) in isotonic Ringer's solution was not markedly influenced by low conductance or by hypertonic Ringer's solution (Tables II–IV). Capacitances as high as 55  $\mu\text{F}/\text{cm}^2$  have been reported in biological tissues (Fatt, 1964), and are thought to represent polarization capacitances (Schwarz, 1962). Hence a distinctive feature of model A would be the attribution of significant electrical characteristics to the intercellular material situated in or very close to the intercellular junctions, i.e., in parallel with the perineurial cells. This is consistent with the electron microscopic demonstration that perineurial cells, instead of being cuboidal with minimum overlap between adjacent cells, are thin flattened cells with extensive lateral overlap (Shinowara et al., 1982).

On the other hand, in model B,  $R_2$  and  $C_2$  would arise at membranes of the perineurial cells with  $R_2$  being the cell membrane resistance shunted by the junctional resistance, and  $R_1$  and  $C_1$  then would represent the intercellular material between and in series with the perineurial cell layers. The connective tissue space between the cell layers contains collagen fibers and amorphous ground substance with embedded small fibrillar elements. This matrix is intimately related to the adjacent cell layers and often extends into the invaginations and calveoli of the cell membranes (Shinowara et al., 1982). Exposure to low conductance Ringer's solution, which should affect primarily the intercellular conductivity, elevated  $R_1$  and  $R_2$  by 4–5 times, consistent with the above interpretation, but did not markedly affect  $C_1$  and  $C_2$ . Hypertonic exposure, followed by return to isotonic Ringer's solution, reduced both  $R_1$  and  $R_2$ , consistent with observations on  $^{14}\text{C}$ -sucrose permeability (Weerasuriya et al., 1979a).

With the exception of the foregoing comments, there is no morphological reason to exclude either model A or B. Whereas model A stresses the electrical properties of the

extracellular matrix in parallel with perineurial cells, model B emphasizes structures between perineurial cell layers. Both are consistent with the known ultrastructure of the perineurium. A choice of one or the other model must await further information, such as microelectrode recordings of potential distribution within the perineurium, and experimental manipulations of selected layers of the perineurium.

Models C and D, on the other hand, are difficult to relate to the known structure of the perineurium. In model D, for example,  $C_2$ , representing the capacitance of the cell membranes, does not have in parallel a resistor that should represent the junctional and cell membrane resistance. In model C, even though the parallel arrangement of  $R_1$  and  $C_1$  agrees with what is expected of cell membranes, the presence of  $C_2$  in series with  $R_1$  and  $C_1$  would prevent expression of cell membrane and junctional resistance,  $R_1$ , in a DC measurement. Because of these limitations, models C and D do not seem appropriate.

Our estimate of DC resistance compares favorably with the 300–500  $\Omega\text{cm}^2$  reported by earlier AC (Cole and Curtis, 1936; Rashbass and Rushton, 1949; Taylor, 1950) and DC (Nicely, 1955) measurements of the frog sciatic nerve perineurium. It is at the lower end of resistances of nonleaky epithelia, which range from 500 to 3,800  $\Omega\text{cm}^2$  (Frömter and Diamond, 1972; Crone and Olesen, 1982), but higher than resistances of leaky epithelia at 20°C, which may range from 73 to 113  $\Omega\text{cm}^2$ . These observations, and measurements of perineurial  $\text{Na}^+$  permeability and hydraulic conductivity (see Introduction), indicate that the perineurium of the frog sciatic nerve has properties intermediate between those of leaky and nonleaky epithelia (Frömter and Diamond, 1972).

The absence of a measurable transperineurial potential difference characterizes several leaky epithelia in which active transport has been demonstrated (Frömter and Diamond, 1972; Rapoport, 1976), but in view of symmetric and ouabain-independent fluxes of  $\text{Na}^+$  and  $\text{K}^+$  at the perineurium (Weerasuriya et al., 1980), it is highly probable that ions are not actively transported by the in vitro perineurium. In the absence of electrochemical gradients, the conductance ( $g_i$ ) of an univalent ion across a two-dimensional barrier is related to its permeability ( $P_i$ ) by  $g_i = (P_i F^2 C_i) / RT$  where  $R$  is the gas constant,  $T$  is the temperature,  $F$  is Faraday, and  $C_i$  is the concentration of that ion. By inserting measured permeability coefficients of Na, Cl, and K (Weerasuriya et al., 1980) in the above equation, the individual conductances of these ions can be calculated. The inverse of the sum of their conductances yields a transperineurial DC resistance of 580  $\Omega\text{cm}^2$  which compares quite favorably with the 478  $\Omega\text{cm}^2$  reported in this investigation.

Exposure of the perineurium to a low conductance medium increased the DC resistance. Because this increase was reversed by returning tissue to normal Ringer's solution, it probably resulted from permeation of the low-

conductance solution into the intercellular matrix and the junctional regions. This medium also produced a decrease of the membrane capacitance though it could not be shown to be statistically significant. Adrian and Almers (1974) noticed a similar decrease in the effective capacitance of frog skeletal muscles when subjected to a low-conductance medium.

We thank Dr. Harold Lecar for helpful discussions, Mr. Herbert Walters for assistance in the fabrication of the instruments, and Mrs. Maxine Schaefer and Mrs. Johnnie James for secretarial assistance. We also thank the referees for their critical comments, which significantly improved the manuscript.

Received for publication 27 June 1983 and in final form 9 April 1984.

## REFERENCES

- Ask, P., H. Levitan, P. J. Robinson, and S. I. Rapoport. 1983. Peripheral nerve as an osmometer: role of the perineurium in frog sciatic nerve. *Am. J. Physiol.* 244:C75–C81.
- Adrian, R. H., and W. Almers. 1974. Membrane capacity measurements on frog skeletal muscle in media of low ion content. *J. Physiol. (Lond.)* 237:573–605.
- Akert, K., C. Sandri, E. R. Weibel, K. Peper, and H. Moor. 1976. The fine structure of the perineurial endothelium. *Cell Tissue Res.* 165: 281–295.
- Brown, A. C., and K. G. Kastella. 1965. The AC impedance of frog skin and its relation to active transport. *Biophys. J.* 5:591–606.
- Burkel, W. E. 1967. The histological fine structure of the perineurium. *Anat. Rec.* 158:177–190.
- Claude, P., and D. A. Goodenough. 1973. Fracture faces of zonulae occludentes from "tight" and "leaky" epithelia. *J. Cell Biol.* 58:390–400.
- Clausen, C., S. A. Lewis, and J. M. Diamond. 1979. Impedance analysis of a tight epithelium using a distributed resistance model. *Biophys. J.* 26:291–318.
- Clausen, C., T. E. Machen, and J. M. Diamond. 1983. Use of AC impedance analysis to study membrane changes related to acid secretion in amphibian gastric mucosa. *Biophys. J.* 41:167–178.
- Cole, K. S., and H. J. Curtis. 1936. Electrical impedance of nerve and muscle. *Cold Spring Harbor Symp. Quant. Biol.* 4:73–113.
- Crescitelli, F. 1951. Nerve sheath as a barrier to the action of certain substances. *Am. J. Physiol.* 166:229–240.
- Crone, C., and S. P. Olesen. 1982. Electrical resistance of brain microvascular endothelium. *Brain Res.* 24:49–55.
- Erlj, D., and A. Martinez-Palomo. 1972. Opening of tight junctions in the frog skin by hypertonic urea solutions. *J. Membr. Biol.* 9:229–240.
- Falk, G., and Fatt, P. 1964. Linear electrical properties of striated muscle fibres observed with intracellular electrodes. *Proc. R. Soc. (Lond.) B. Biol. Sci.* 160:69–123.
- Fatt, P. 1964. An analysis of the transverse electrical impedance of striated muscle. *Proc. R. Soc. (Lond.) B. Biol. Sci.* 159:606–651.
- Feng, T. P., and Y. M. Liu. 1949. The connective tissue sheath of the nerve as an effective diffusion barrier. *J. Cell Comp. Physiol.* 34: 1–16.
- Finn, A. L., and J. Bright. 1978. The paracellular pathway in toad urinary bladder. *J. Membr. Biol.* 44:67–83.
- Freygang, W. H., and W. Trautwein. 1970. The structural implications of the linear electrical properties of cardiac Purkinje strands. *J. Gen. Physiol.* 55:524–547.
- Frömter, E., and J. Diamond. 1972. Routes of passive ion permeation in epithelia. *Nature (Lond.)* 235:9–13.
- Knott, G. D. 1979. M Lab — a mathematical modeling tool. *Comput. Programs Biomed.* 10:271–280.

- Krnjevic, K. 1954. Some observations on perfused frog sciatic nerve. *J. Physiol. (Lond.)* 123:338-356.
- Lane, N. J. 1981. Invertebrate neuroglia-junctional structure and development. *J. Exp. Biol.* 95:7-33.
- Low, F. N. 1976. The perineurium and connective tissue of peripheral nerve. In *The Peripheral Nerve*. D. N. Landon, editor. Chapman and Hall, London. 159-187.
- Nicely, M. 1955. Measurement of the potential difference across the connective tissue sheath of frog sciatic nerve. *Experientia (Basel)* 11:199-200.
- Olsson, Y., and T. S. Reese. 1971. Permeability of vasa nervorum and perineurium studied by fluorescence and electron microscopy. *J. Neuropathol. Exp. Neurol.* 30:105-119.
- Rapoport, S. I. 1976. *Blood-Brain Barrier in Physiology and Medicine*. Raven Press, New York. 316.
- Rashbass, C., and W. A. H. Rushton. 1949. The relation of structure to the spread of excitation in the frog's sciatic trunk. *J. Physiol. (Lond.)* 110:110-135.
- Rawlins, F. A., E. Gonzales, M. Renez-Gonzales, and G. Whittembury. 1975. Effect of transtubular osmotic gradients on the paracellular pathway in toad kidney proximal tubule. *Pfluegers Arch. Eur. J. Physiol.* 377:125-133.
- Reale, E., L. Luciano, and M. Spitznas. 1975. Freeze-fracture faces of the perineurial sheath of the rabbit sciatic nerve. *J. Neurocytol.* 4:261-270.
- Schifferdecker, E., and E. Frömter. 1978. The AC impedancy of Necturus gallbladder epithelium. *Pfluegers Arch. Eur. J. Physiol.* 377:125-133.
- Shinowara, N., M. E. Michel, and S. I. Rapoport. 1982. Morphological correlates of permeability in the frog perineurium: vesicles and "trans-cellular channels." *Cell Tissue Res.* 227:11-22.
- Schwarz, B. 1962. A theory of the low-frequency dielectric dispersion of colloidal particles in electrolyte solutions. *J. Phys. Chem.* 66:2636-2642.
- Smith, P. G. 1975. Frequency dependence of the frog skin impedance. *Biochim. Biophys. Acta.* 375:124-129.
- Spring, K., and G. Giebisch. 1977. Tracer fluxes in necturus proximal tubule. *Am. J. Physiol.* 232:F461-F470.
- Taylor, R. E. 1950. Studies of the Effect of Externally Applied Currents on Frog Nerve. Ph.D. Thesis, University of Rochester, Rochester, NY.
- Thomas, P. K., and Y. Olsson. 1975. Microscopic anatomy and function of the connective tissue components of peripheral nerve. In *Peripheral Neuropathy*. J. Dyck, P. K. Thomas, and P. W. Lampert, editors. Saunders, Philadelphia, PA. 168-189.
- Tomita, T. 1969. The longitudinal tissue impedance of the smooth muscle of guinea-pig *Taenia coli*. *J. Physiol. (Lond.)* 201:145-159.
- Ussing, H. H. 1966. Anomalous transport of electrolytes and sucrose through the isolated frog skin induced by hypertonicity of the outside bathing solution. *Ann. NY Acad. Sci.* 137:543-555.
- Valdiosera, R., C. Clausen, and R. S. Eisenberg. 1974. Impedance of frog skeletal muscle fibers in various solutions. *J. Gen. Physiol.* 63:460-491.
- Waggenger, J. D., S. M. Bunn, and J. Beggs. 1965. The diffusion of ferritin within the peripheral nerve sheath: an electron microscopy study. *J. Neuropathol. Exp. Neurol.* 24:430-443.
- Weerasuriya, A., S. I. Rapoport, and R. E. Taylor. 1979a. Modification of permeability of frog perineurium to <sup>14</sup>C-sucrose by stretch and hypertonicity. *Brain Res.* 173:503-512.
- Weerasuriya, A., R. A. Spangler, S. I. Rapoport, and R. E. Taylor. 1979b. Electrical impedance of the perineurium of the frog sciatic nerve. *Biophys. J.* 25(2, Pt. 2):300a. (Abstr.)
- Weerasuriya, A., S. I. Rapoport, and R. E. Taylor. 1980. Ionic permeabilities of the frog perineurium. *Brain Res.* 191:405-415.